EP Note 4

ENVIRONMENTAL PROTECTION NOTE #4

SOIL ACTIVATION UNDER THE P EAST TARGET BOX

S.I. Baker

July 26, 1976

Table of Contents

Tables

Figures

SUMMARY

Measurements of radioactivity near the Proton East Target Box indicated a shielding capability 40 per cent of that predicted. As expected, the present amount of soil activation was no hazard. An average intensity during 1975 of five per cent of the maximum capability accounted for the low soil activation. The technique used in the measurements was a simple and inexpensive one. Radioactivity was measured in copper and aluminum tags on top of the target box. These results yielded soil ^{22}Na concentrations after the application of suitable correction factors: a conversion factor from tag to soil concentrations and attenuation factors for the additional shielding thicknesses. An integration was then performed to obtain the total soil ^{22}Na activity.

Recommendations were made for further tests and for improving the shielding.

1. INTRODUCTION

I determined radioactivity in the soil under the Proton East (P East) Target Box to answer two questions:

1. Is the present amount of soil activation hazardous?
2. Is the shielding of the soil adequate for around-the-clock operation at the original design's maximum intensity of 2×10^{12} protons per second on target?[1]

Since the total number of protons delivered to the P East target during 1975 was only two per cent of the designed maximum per year, I expected a "No" answer to the first question. No one had considered the second question. I decided to look for the answer because the proton beam intensity recently reached about 40 per cent of the design intensity for brief periods and extended operations at even higher intensities is possible.

Since the total number of protons on target has been small, I did not believe an expensive soil boring operation, such as was done in the Neutrino Area, was warranted for the P East Target Box. Instead, I conducted a simple, inexpensive activation measurement using copper and aluminum tags (Section 2). The ^{22}Na concentration in an aluminum tag is easily related to the concentration of ^{22}Na in Fermilab soil at the same location.[2] That radionuclide and ^{3}H (tritium) are the two long-lived activities leachable from Fermilab soils. Limits are available for safe annual production of them on site in unprotected soil.[3] A measurement of either activity is sufficient to determine a potential hazard.

I converted the tag results to activities in the soil using a previously established ratio and then calculated the activities at other soil depths using the rate of change in activity with distance predicted by a model. I summed up all the contributions to get the total activity (Section 3) and determined the maximum number of protons per second for safe around-the-clock operation with the existing shielding. I then converted the total activity in the soil to that for the original design shielding and calculated the corresponding maximum permissible intensity. I compared that maximum with the value obtained in the original design calculation and made recommendations for future work (Section 6).

2. TAG ACTIVATION MEASUREMENT

To avoid the expense of soil borings to determine soil activation, I placed aluminum and copper disks (tags) on top of the P East Target Box (Fig. 1). These were irradiated from May 12 to July 7, 1975, by secondary particles from the interaction of 2×10^{17} protons (total) in the target box. Because the steel shielding in the target box limited accurate measurements of ^{22}Na in aluminum to a few locations, copper tag results were used to obtain concentrations by the following technique:

1. The ^{54}Mn activity was measured in each copper tag (Fig. 2). That radionuclide has a shorter half-life than ^{22}Na (310 days compared to 950 days for ^{22}Na). However, the period of irradiation was sufficiently short (56 days) that the error introduced by radioactive decay during the irradiation was small, about ten per cent. The somewhat higher threshold for ^{54}Mn production

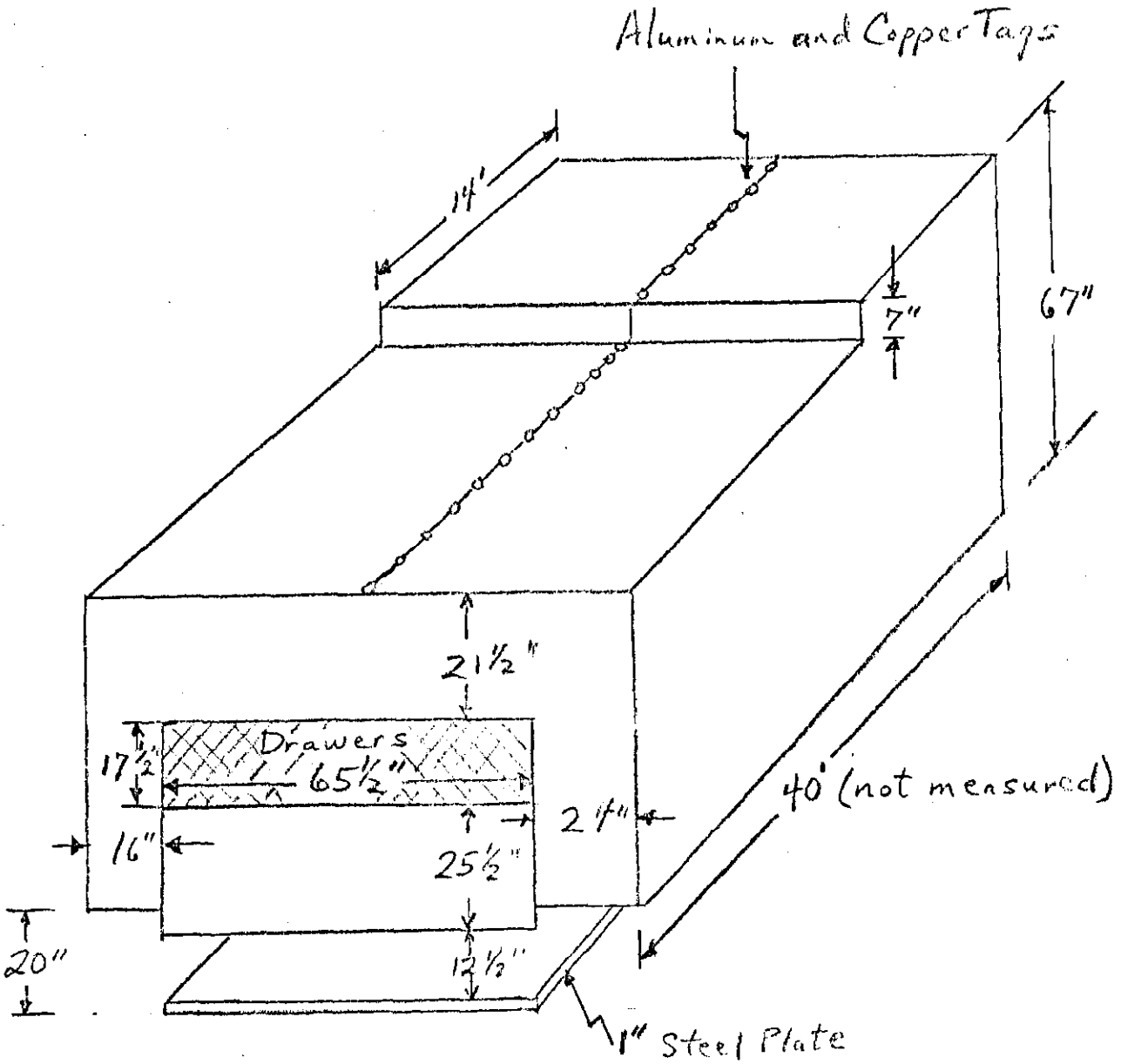

Figure 1. Actual Shielding for PEast Target Box

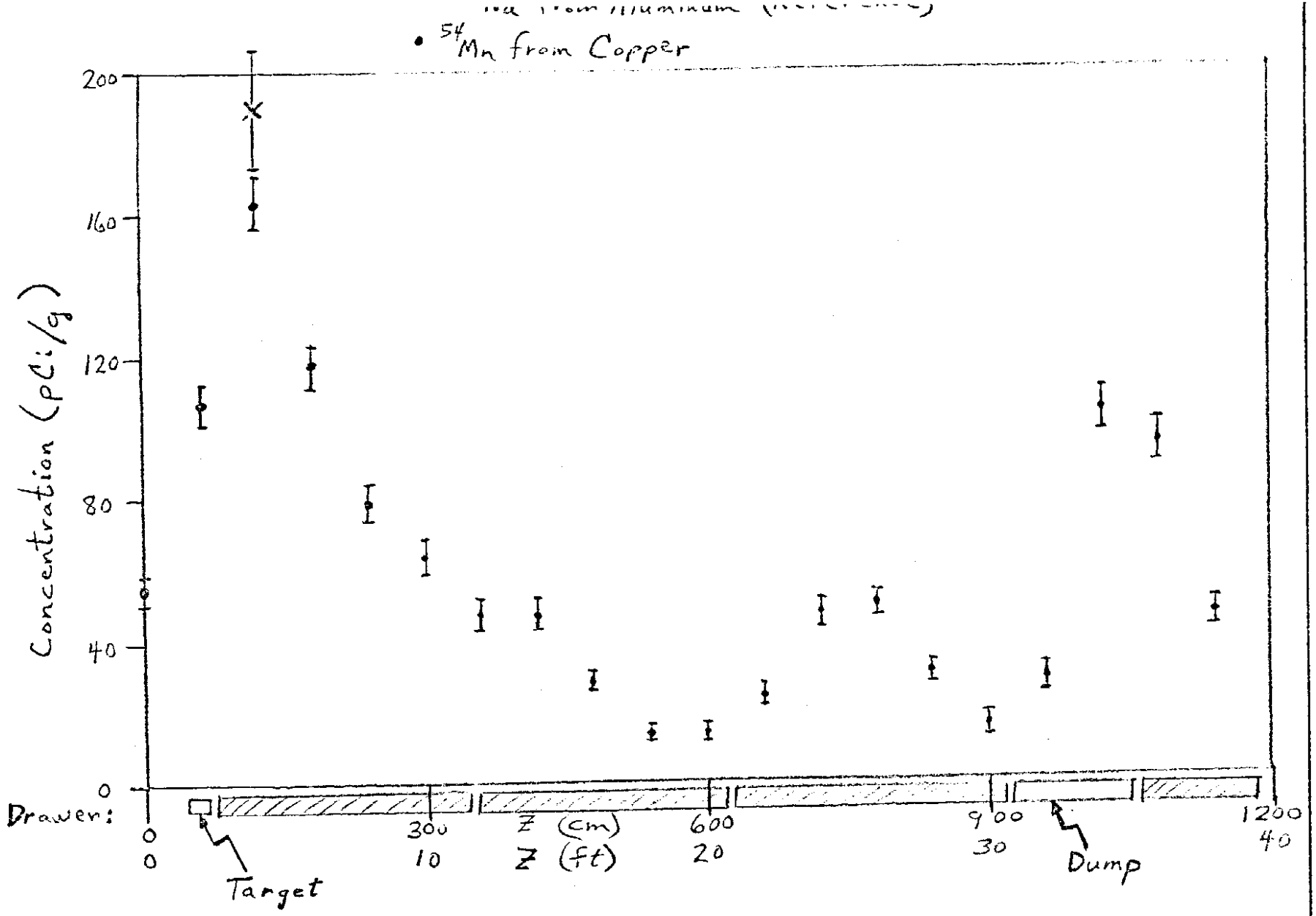

Figure 2. PEast Target Box Drawer Configuration and Tag Results

in copper compared with ^{22}Na in aluminum also introduced some error.[4,5]

2. The ratio between ^{54}Mn in copper and ^{22}Na in aluminum was determined at the point of highest activation.

3. The ratio at the point of highest activation was used to calculate ^{22}Na concentrations from the measurements of ^{54}Mn activity at other locations (Table 1).

4. Each aluminum ^{22}Na concentration resulting from the preceding step was then converted to a ^{22}Na concentration in Fermilab soil at the same location by dividing by 3.34, a constant determined in a previous measurement.[2]

3. DETERMINATION OF TOTAL SOIL ACTIVITY

3.1 Concentrations Under the Target Box

To get the total amount of ^{22}Na in the soil from the tag measurements, we next determined concentrations just below the target box. I measured the thickness of steel in the box to see if a correction was needed for differences in steel thickness above and below the target box. Except for the last 14 feet, the thickness of the target box was four inches greater below the target than above. The thickness was three inches less for the last 14 feet. To determine the corrections for the differences in thickness, I used the nuclear cascade model that A. Van Ginneken uses.[6] Then I obtained concentrations in the soil below the 20-inch thick concrete floor using the same technique and replacing the concrete by its equivalent for shielding purposes--20 cm of iron.[7] The details are shown in Appendix 1 and the results are given in Table 2.

Table 1. ^{22}Na Soil Concentrations at Tag Locations

Distance From Front of Target Box (cm)	Concentrations (pCi/g)			
	^{54}Mn in Cu measured	^{22}Na in Al measured	^{22}Na in Al calculated	^{22}Na in Fermilab Soil calculated*
0	55 ± 4		64	19
60	107 ± 6	135 ± 14	124	37
120	164 ± 7	190 ± 17	190	57
180	118 ± 6	171 ± 16	137	41
240	79 ± 5	89 ± 12	92	28
300	63 ± 5		73	22
360	48 ± 4		56	17
420	48 ± 4		56	17
480	29 ± 3		34	10
540	14 ± 2		16	5
600	14 ± 2		16	5
660	24 ± 3		28	8
720	47 ± 4		54	16
780	49 ± 4		57	17
840	30 ± 3		35	10
900	15 ± 3		17	5
960	28 ± 4	34 ± 7	32	10
1020	103 ± 6	129 ± 14	119	36
1080	94 ± 6	79 ± 11	109	33
1140	46 ± 4	46 ± 8	53	16

*Concentration in aluminum ÷ 3.34

Table 2. ^{22}Na Concentrations in the Soil Adjacent to the Target Box

Distance Z from Front End of Target Box (cm)	^{22}Na Soil Concentrations Just Outside Concrete Enclosure							
	Underneath		West Side		Above		East Side	
	pCi/g	pCi/cm^3 $S_1(Z)$	pCi/g	pCi/cm^3 $S_2(Z)$	pCi/g	pCi/cm^3 $S_3(Z)$	pCi/g	pCi/cm^3 $S_4(Z)$
0	1.9	4.6	0.19	0.46	6.7	16	0.047	0.11
60	3.7	8.9	0.37	0.89	13	31	0.092	0.22
120	14	34	3.4	8.2	30	72	1.5	3.5
180	10	25	2.5	5.9	22	52	1.0	2.5
240	7.9	19	2.2	5.3	15	37	1.0	2.4
300	6.2	15	1.7	4.2	12	29	0.81	1.9
360	4.8	11	1.3	3.2	9.4	23	0.62	1.5
420	4.8	11	1.3	3.2	9.4	23	0.62	1.5
480	2.9	7.0	0.81	1.9	5.7	14	0.38	0.90
540	1.4	3.3	0.38	0.91	2.7	6.5	0.18	0.42
600	1.4	3.3	0.38	0.91	2.7	6.5	0.18	0.42
660	2.4	5.7	0.67	1.6	4.7	11	0.31	0.74
720	4.6	22	1.3	3.1	9.1	22	0.60	1.4
780	4.9	23	1.4	3.3	9.6	23	0.63	1.5
840	3.0	14	0.83	2.0	5.9	14	0.39	0.93
900	1.5	6.9	0.40	0.97	2.9	6.9	0.19	0.45
960	2.7	13	0.76	1.8	5.4	13	0.35	0.85
1020	10	48	2.8	6.8	20	48	1.3	3.2
1080	9.3	44	2.6	6.2	18	44	1.2	2.9
1140	4.5	21	1.3	3.0	8.9	21	0.59	1.4

3.2 Attenuation in the Soil

Since the elemental compositions of soil and concrete are similar, I assumed that the total production of ^{22}Na in them is equal. Then I used the curves of Van Ginneken for concrete to determine the decrease in ^{22}Na production with depth in the soil. Using the curves (Fig. 3), I found that this decrease, or attenuation, could be represented by an exponential function. For radial distances r corresponding to locations in the soil beneath the target box the exponential takes the form $\exp\left[-0.0307\ (r - R_o)\right]$, where r and R_o are the distances from the target axis to the point in question and to the top of the soil, respectively (Fig. 4).

3.3 Lateral Decrease

At a fixed depth below the target box the soil activation decreases as one moves laterally from the vertical centerline of the target. I measured the rate of decrease earlier using a set of tags under the target box (Fig. 5).[8] The relative activity went from 1 to 0.7 to 0.35 as the lateral distance from the target went from 0 to 1.5 to 3 feet. The exponential form in Section 3.2 above represented the lateral decrease well (Appendix 2).

3.4 Integration

To obtain the total activity "I" in the soil, I integrated the equation[7]

$$I = \int_{z=0}^{\infty} dz \int_{\varphi=0}^{2\pi} d\varphi \int_{r=R_o(\varphi)}^{\infty} S(z, r, \varphi)\, r\, dr \qquad (1)$$

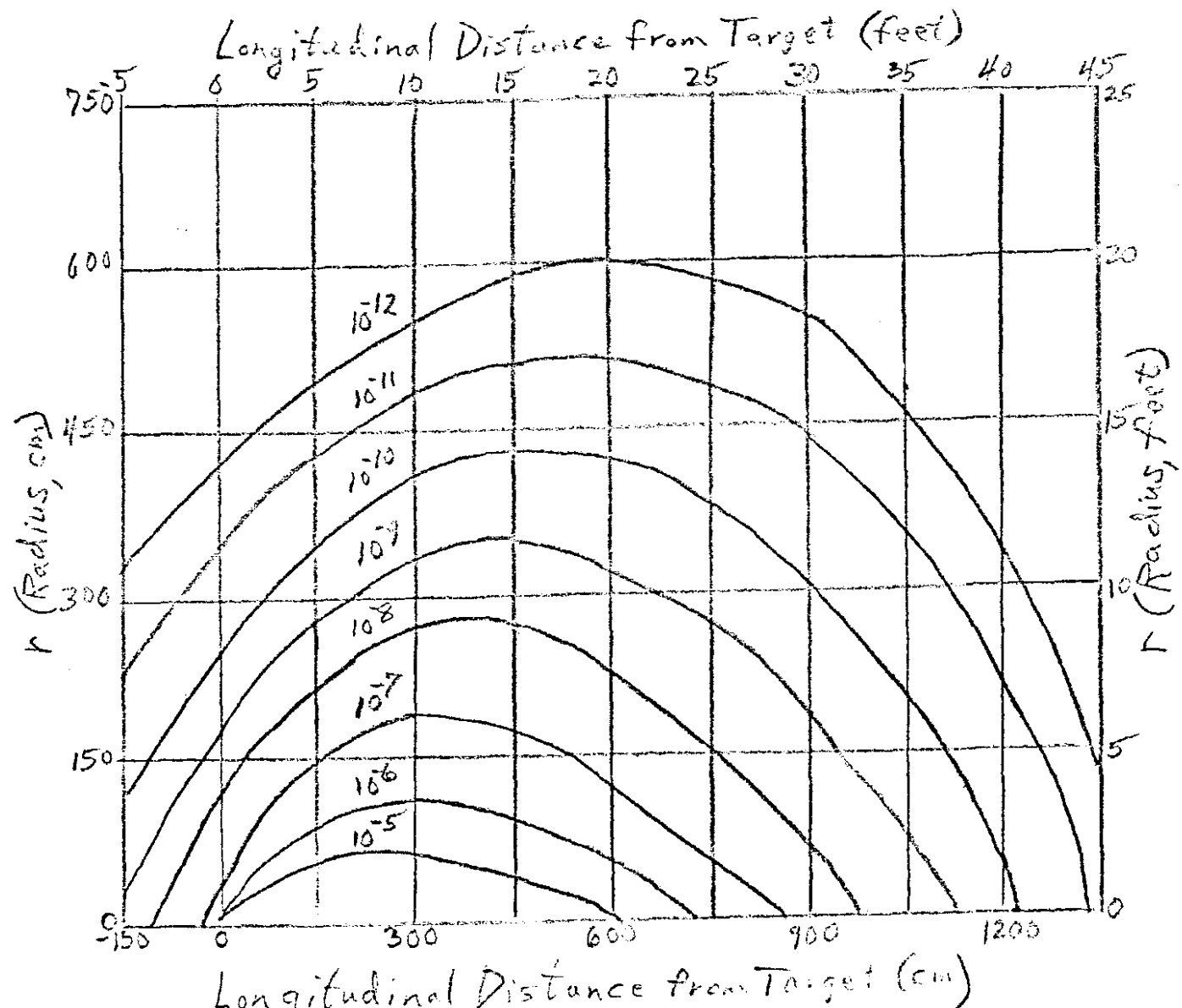

Figure 3. 300 GeV protons incident on a solid concrete cylinder. Contours of equal star density (stars/cm³ and incident proton). The ^{22}Na

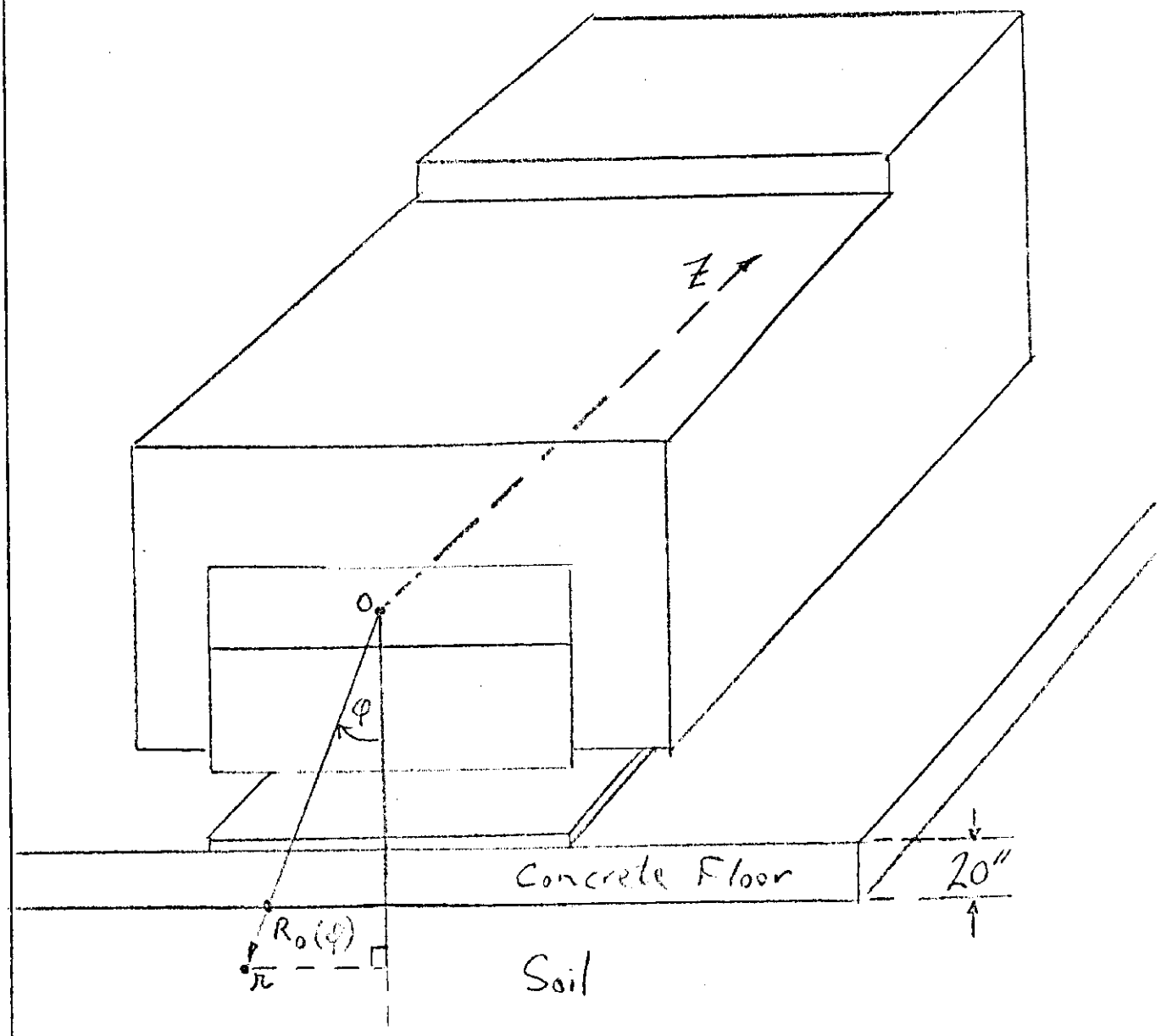

Figure 4. Geometry for PEast Target Box

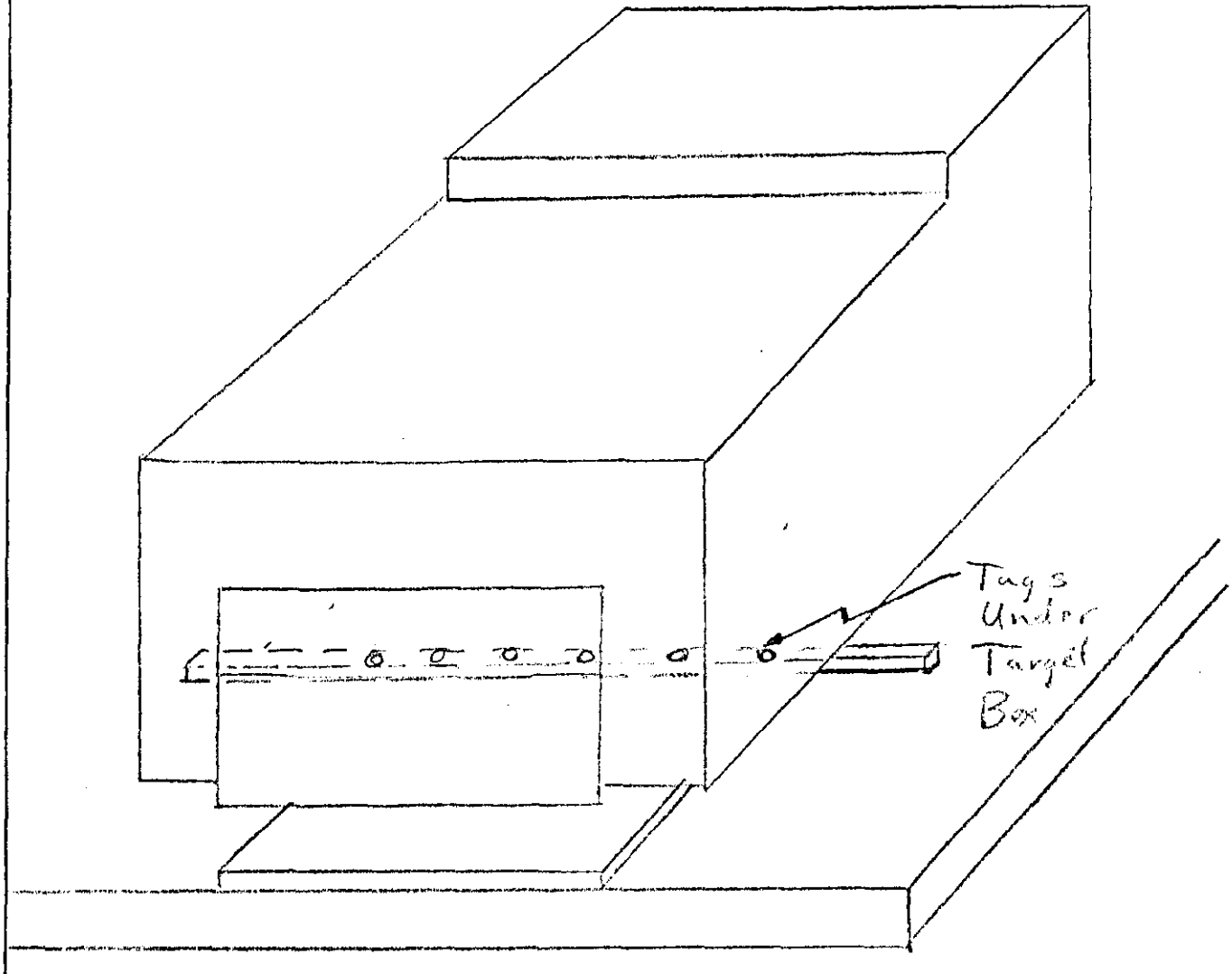

Figure 5. Measurement of Lateral Decrease

Expressed in terms of the exponential decrease (Section 3.2 above), the function S (z,r,φ) became

$$S(z, r, \varphi) = S(z, \varphi)\ e^{-0.0307[r - R_o(\varphi)]}$$

where S (z,φ) is the concentration in pCi/g at the longitudinal distance z from the front of the target box (Fig. 4). The lateral decrease (Section 3.3 above) is explicitly shown by writing $S(z,\varphi)$ as

$$S(z, \varphi) = S_j(z)\, M(\varphi)\ e^{-0.0307[r, R_o(\varphi)]}$$

where M (φ) is a multiplier to convert from the value of $S_j(z)$ at $\varphi = 0$ to the value at the desired value of φ (Appendix 2).

The longitudinal integration can be carried beyond the target box (z greater than 1140 cm). The activation decreases about ten times for every 150 cm increase in z for z greater than 1140 cm and for values of r corresponding to locations in the soil (r greater than 140 cm). See Fig. 3. Thus, the exponential decrease is represented by

$$S_j(z) = S_j(1140)\ e^{-0.0154(z - 1140)} \qquad , z > 1140 \text{ cm.}$$

3.5 Result of Integration

The details of the integration are shown in Appendix 3. The result using the concentrations given in Table 2 for $S_j(z)$ at $\varphi = 0$ is

$$I = 3.9 \times 10^8 \text{ pCi or } 390 \mu\text{Ci of } {}^{22}\text{Na}.$$

The uncertainty in the calculation just from the approximations made in using the curves of Van Ginneken and in integrating is estimated to be 30 per cent. The uncertainties in the ^{22}Na concentrations in

soil at the tag locations are also about 30 per cent.

4. MODEL PREDICTIONS

4.1 Nuclear Cascade Model

I used the nuclear cascade model directly to get the ^{22}Na concentration in the soil. This model starts with a proton incident on the target and traces the resulting cascade of secondary particles using a Monte Carlo technique. A. Van Ginneken has found that the number of nuclear interactions (stars) per cubic centimeter at large radial distances from the primary proton interaction (r greater than 50 cm in iron) obeys the relation[5]

$$S(z,r) = 50\,\frac{S(z,50)}{r}\,e^{-\frac{(r-50)}{\lambda_r(z)}}.$$

4.2 Application to Design Shielding

Van Ginneken substituted the above relation for $S(z, r, \varphi)$ in Equation 1 above and used the expression

$$\lambda_r(z) = 13.6 + 0.047\,Z$$

for the iron in the target box. He also assumed that the voids under and above the target box would be filled with steel (Fig. 1). He calculated the total number of stars for the design shielding and obtained 0.072 stars per incident proton in unprotected soil outside the shielding or a maximum of 2.1×10^{12} protons/sec for around-the-clock operation. The latter number was obtained using the criterion that 0.0152 stars per incident proton will produce 42 mCi of ^{22}Na per year in unprotected soil for around-the-clock operation with 10^{13} protons

per second striking the target.[2,7]

4.3 Application to Shielding As Built

Since the Proton East Target Box was built with less steel than the design called for, I repeated the above integration for the steel used in the design calculation (Appendix 4). For comparison with Van Ginneken's result I neglected the contributions beyond the end of the target box (about 10 per cent) and obtained a maximum of 8.5×10^{11} protons/sec for around-the-clock operation.

5. COMPARISON OF EXPERIMENTAL AND MODEL RESULTS

The ^{22}Na activity produced in the soil was obtained by three methods:

1. An experiment gave measurements in aluminum and copper tags. These results were used to calculate the activity for a given number of protons on target.

2. A design called for a certain amount of steel. A model had been used to find the number of protons on target to give 42 mCi of ^{22}Na.

3. A measurement of the amount of steel in the target box as built revealed less than specified in the original design. Thus, the results from the tag measurements could not be compared directly with the design calculation. I repeated the integration for the steel used in the design calculation and determined the number of protons required to give 42 mCi of ^{22}Na.

The three results appear in Table 3. The results show that the maximum permissible proton intensity for around-the-clock operation is one-third the design value.

Table 3. Comparison of Maximum Intensities

	Maximum Permissible Intensity (protons/sec)
1. Experiment for As Built Shielding	0.7×10^{12}
2. Design Calculation	2.1×10^{12}
3. Experimental Results Applied to Design Shielding	0.9×10^{12}

The average number of protons per second incident on the target for 1975 was 3.7×10^{10} protons/sec, or approximately five per cent of the lowest limit in Table 3. For the preceding years it was even lower. From those results I conclude that the ^{22}Na activity in the soil at the end of 1975 presents no radiation hazard.

6. RECOMMENDATIONS

The discrepancy between the experimental and design calculation (Table 3) indicates a need for further tests. I recommend the following:

1. Make a Monte Carlo calculation, using the same model, to calculate the activities in the tags and the total activity in the soil. Do the calculation in detail with the best possible representation of the target box and its contents.

2. Add steel to permit operation around-the-clock at 2×10^{12} protons per second. Steel should be added first under the target box since there are no underdrains below the enclosure floor. The underdrains around the enclosure footings collect some water from the sides and top of the enclosure. Hence, they should reduce the hazard from ^{22}Na leached from the soil above and to the side.

3. Make a set of soil borings to determine the activity directly.

I believe the first recommendation should be implemented this year. The steel should be added and the soil borings made before the proton intensity for around-the-clock operation exceeds 30 per cent of the lowest limit in Table 3. This would provide an extra margin of safety.

7. REFERENCES

1. Memo from Miguel Awschalom to Linc Read and Dave Eartly on Oct. 3, 1972.

2. Soil Activation Log #1, p. 134.

3. Miguel Awschalom, Fermilab Internal Report TM-292, 1971.

4. H. R. Heydegger et al., Phys. Rev. C6, 1235 (1972).

5. J. B. Cumming, Annual Reviews of Nuclear Science 13, 261 (1963).

6. A. Van Ginneken and M. Awschalom, High Energy Particle Interactions in Large Targets, Vol. 1, Fermi National Accelerator Laboratory, ca. 1975.

7. Memo from Miguel Awschalom to Linc Read on Sept. 5, 1972.

8. Soil Activation Log #1, pp. 42 and 124.

9. M. Awschalom et al., Fermilab Internal Report TM-168, 1969.

Appendix 1. CORRECTIONS FOR THICKNESS DIFFERENCES

The target box measurements revealed that the steel thickness was not the same above and below the target. For the first 26 feet (780 cm) the shielding above the target was 77 cm thick and for the last 14 feet it was 95 cm. The steel below the target was 90 cm thick for the entire length of the box; however, there was an additional 50 cm (20 inches) of concrete between the steel and the soil. This amount of concrete is equivalent to 20 cm of iron or steel for shielding purposes[5], making a total of 110 cm below the target.

We wish to determine the ^{22}Na activity in the soil underneath the target box from the tag results above it. Since steel reduces the ^{22}Na production, we must, therefore, correct for the difference in steel thickness. The effect of steel on ^{22}Na production is shown in Fig. 6 for 300 GeV protons striking iron. These curves resulted from a Monte Carlo calculation by A. Van Ginneken[4] which simulated the development of the nuclear cascade. Note the decrease with thickness in the region from 75 to 100 cm radially from the target. This region corresponds to the location of the tags since the target was in the center of the cross-hatched region labeled "Drawers" in Fig. 1.

From Fig. 6 the decrease in ^{22}Na activity with radial distance depends somewhat on the longitudinal position (value of z). From the change in thickness required to give a decrease of ten times (attenuation factor f of ten), I obtained an attenuation coefficient μ. For example, after the first ten feet (300 cm) the thickness required is 60 cm, yielding the equation

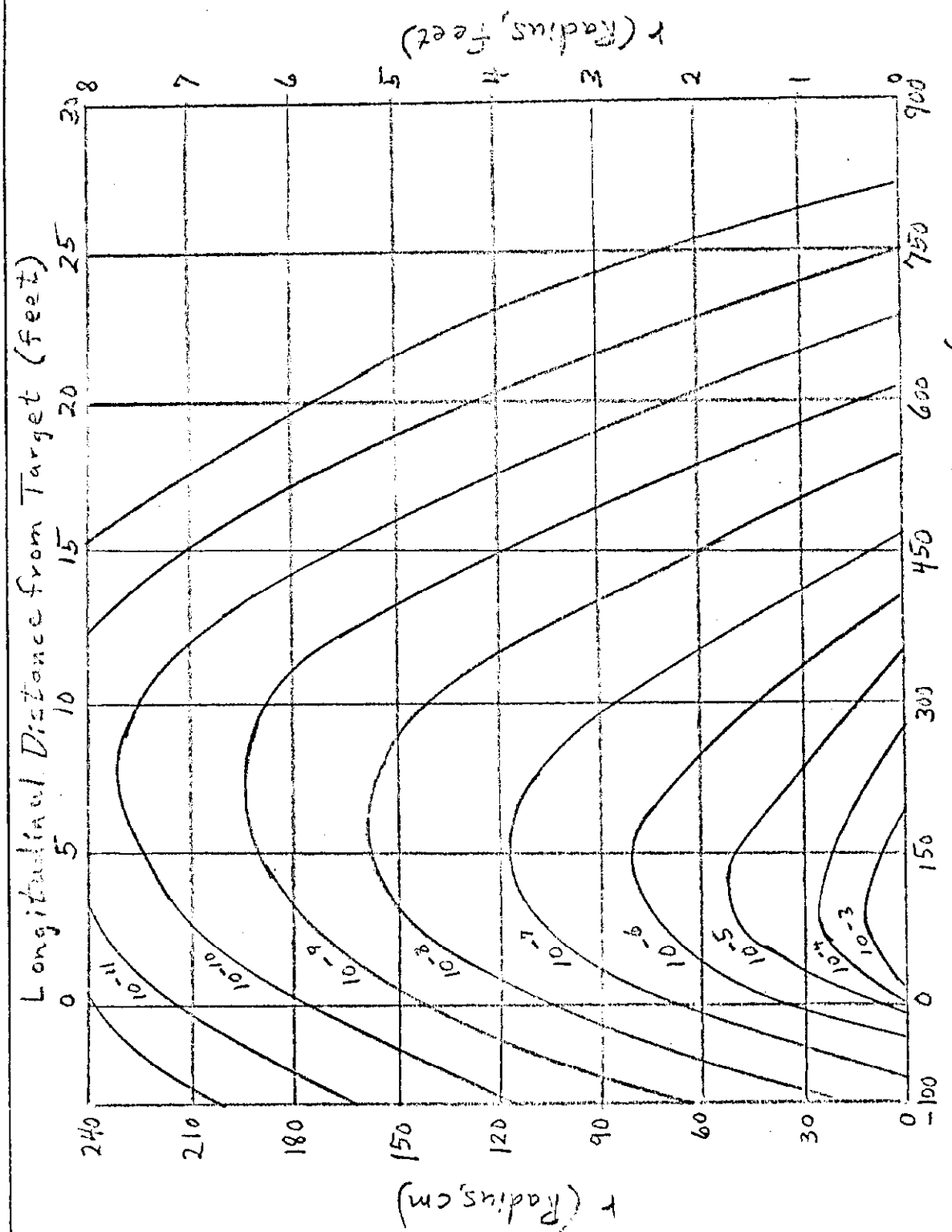

Figure 6. 300 GeV protons incident on a solid iron cylinder. Contours of equal star density (stars/cm³ and incident proton).

$$\frac{1}{f} = 0.1 = e^{-\mu (60\,cm)}$$

and the attenuation coefficient

$$\mu = 0.0384.$$

Using the attenuation coefficients and the thickness differences (33 cm to z = 720 cm and 15 cm for z greater than 720 cm), I obtained the attenuation factors given in Table A1.1. The concentrations in Table 1 were divided by these attenuation factors to obtain the ^{22}Na concentrations in the soil just under the concrete (Table 2).

The same technique was used to find the soil activities just outside the concrete on the sides and above the target box. The equivalent thickness of steel on the west side was 143 cm and on the east side was 163 cm. On top the concrete was 15 inches thick, giving an additional steel thickness of 15 cm.[7] The resulting soil concentrations just outside the concrete are given in Table 2. Since the total activity was calculated using curves based on attenuation in ordinary concrete, the concentration in pCi/cm^3 needed for that integration (Appendix 3) is also given. It was determined using the density 2.4 g/cm^3 for ordinary concrete.[9]

Table A1.1. Attenuation Factors to Convert to Soil Activities Outside the Concrete Enclosure.

Longitudinal Distance Z From Front End of Target Box	Thickness for f = 10	Attenuation Coefficient	Attenuation Factor
(cm)	(cm)	μ	f
0	33	0.06978	10
60	"	"	"
120	54	0.04264	4.084
180	"	"	"
240	60	0.03838	3.548
300	"	"	"
360	"	"	"
420	"	"	"
480	"	"	"
540	"	"	"
600	"	"	"
660	"	"	"
720	"	"	"
780	"	"	1.778
840	"	"	"
900	"	"	"
960	"	"	"
1020	"	"	"
1080	"	"	"
1140	"	"	"

Appendix 2. COMPARISON OF LATERAL DECREASES

The rectangular shape of the target box results in a ^{22}Na decrease as one moves laterally from the centerline to the edge of the box. The increased thickness of steel accounts for this decrease in activity. In an earlier experiment[8] tags were placed underneath the box (Fig. 5) to measure this decrease. The tags were at 45 cm intervals across the box at about 420 cm from the front end. The average of the results (for ^{22}Na in aluminum) on both sides of the centerline showed a decrease in relative activity from 1 to 0.7 to 0.35 as the lateral distance increased from 0 to 45 to 90 cm.

The expected decrease in ^{22}Na production was calculated using the attenuation factor at z = 420 cm from Table A1.1. The exponential evaluated was

$$\exp\{-0.0384[R_o(\varphi)-R_o(0)]\}$$

with $R_o(\varphi)$ as defined in Fig. 4. The results are given in Table A2.1 along with results using the expression

$$M_j(\varphi)=\exp\{-0.0307[R_o(\varphi)-R_o(0)]\}$$

The latter expression was obtained for concrete in Section 3.2. Since it agreed better with experiment and also simplified the integration for total ^{22}Na activity (Appendix A3), the expression with attenuation coefficient 0.0307 was used to represent the lateral decrease.

Using 45 cm steps and the attenuation coefficient 0.0307, I calculated the lateral decreases $M_j(\varphi)$ for the sides and top in the same manner. The results are tabulated in Table A2.2 for the "as built" steel and in Table A2.3 for the design configuration (Fig. 7).

Table A2.1. Comparison of Lateral Decreases

Lateral Distance (cm)	Relative Measured	^{22}Na Activity Calculated $\mu = 0.0384$	$\mu = 0.0307$
0	1.0	1.0	1.0
45	0.7	0.7	0.76
90	0.35	0.29	0.37

Table A2.2. Values of Multiplier Mj(ψ) for "As Built" Target Box.

Location	ψ Interval (radians)	Ro (ψ)	Mj (ψ)
Bottom	- 0.887 to - 0.977	174.1	0.140
j = 1	0.887 to 0.915	"	"
	± 0.686 to ± 0.887	142.1	0.373
	± 0.388 to ± 0.686	118.8	0.762
	0 to ± 0.388	110.0	1.000
West	- 0.562 to 0.656	169.0	0.451
First 26 ft.	± 0.305 to ± 0.562	149.9	0.809
j = 2	0 to ± 0.305	143.0	1.000
West	± 0.562 to ± 0.656	169.0	0.451
Last 14 ft.	± 0.305 to ± 0.562	149.9	0.809
j = 2	0 to ± 0.305	143.0	1.000
Top	- 0.983 to - 1.009	162.2	0.109
First 26 ft.	0.983 to 1.066	"	"
j = 3	± 0.785 to ± 0.983	127.3	0.318
	± 0.463 to ± 0.785	100.6	0.722
	0 to 0.463	90.0	1.000
Top	- 0.887 to - 0.915	174.1	0.140
Last 14 ft.	0.887 to 0.977	"	"
j = 3	± 0.686 to ± 0.887	142.1	0.373
	± 0.388 to ± 0.686	118.8	0.762
	0 to ± 0.388	110.0	1.000
East	0.504 to 0.594	186.2	0.491
First 26 ft.	± 0.269 to ± 0.504	169.1	0.829
j = 4	0 to ± 0.269	163.0	1.000
East	± 0.504 to ± 0.594	186.2	0.491
Last 14 ft.	± 0.269 to ± 0.504	169.1	0.829
j = 4	0 to ± 0.269	163.0	1.000

Table 42.3. Values of Multiplier Mj(ψ) for Design Steel

Location	Interval (radians)	Ro(ψ)	Mj(ψ)
Bottom	± 0.602 to ± 0.7854	158.9	0.424
j = 5	± 0.331 to ± 0.602	138.5	0.794
	0 to ± 0.331	131.0	1.000
West	- 0.602 to - 0.7854	158.9	0.424
j = 5	0.602 to 0.698	"	"
	± 0.331 to ± 0.602	138.5	0.794
	0 to ± 0.331	131.0	1.000
Top	± 0.686 to ± 0.872	142.1	0.373
j = 1	± 0.388 to ± 0.686	118.8	0.762
	0 to ± 0.388	110.0	1.000
East	0.602 to 0.7854	158.9	0.424
j = 5	- 0.602 to - 0.698	"	"
	± 0.331 to ± 0.602	138.5	0.794
	0 to ± 0.331	131.0	1.000

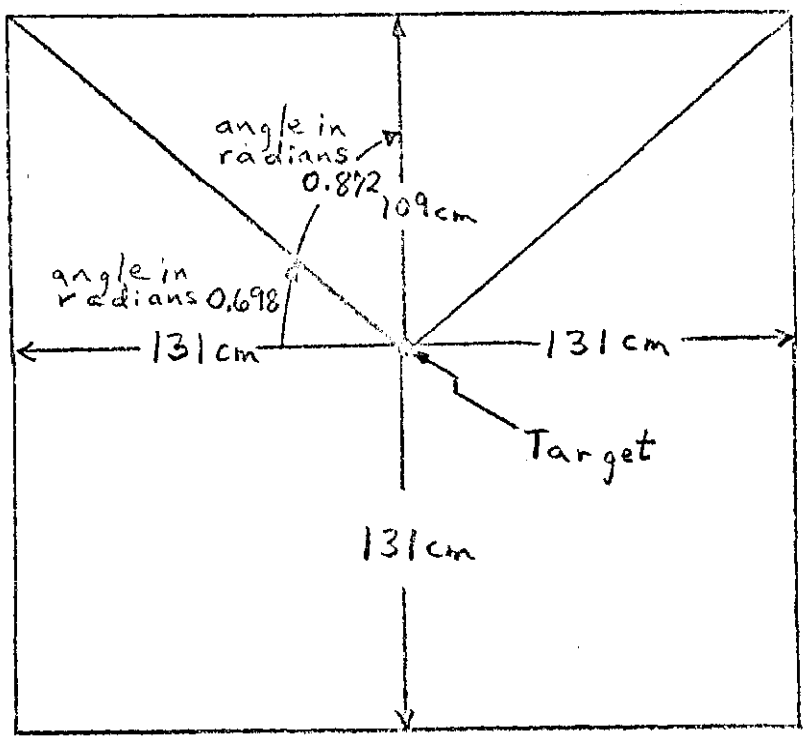

Figure 7. Equivalent Steel Block For Design Calculation

Appendix 3. CALCULATION OF TOTAL ACTIVITY IN SOIL

The rectangular shape of the target box permitted a separation of Equation 1 in Section 3.4 into four sets of equations, one set for each side , one for the top, and one for the bottom of the target box. The concrete enclosure's attenuation was included in the equations by converting the concrete into an equivalent amount of steel.[7] The target drawers were assumed to be solid steel (Fig. 1). The resulting cross sectional views for the equivalent steel box are shown in Fig. 8. Note that the steel is thicker on top for the last 14 feet (Fig. 8b). The details of the integrations to find the total ^{22}Na activity in the soil outside the equivalent steel box are given below.

A3.1 Integration for the First 26 Feet

The equations used for the first 26 feet of the P East Target Box ($0 \leq z < 780$ cm) were as follows:

$$I_{0-26} = \int_{-0.977}^{0.915} d\varphi\, M_1(\varphi) \int_{z=0}^{z=780} dz \int_{r=110\sec\varphi}^{\infty} S_1(z)\, e^{-0.0307(r-110)}\, r\, dr$$

$$+ \int_{\pi/2-0.656}^{\pi/2+0.562} d\varphi\, M_2(\varphi) \int_{z=0}^{z=780} dz \int_{r=143\sec\varphi}^{\infty} S_2(z)\, e^{-0.0307(r-143)}\, r\, dr$$

$$+ \int_{\pi-1.009}^{\pi+1.066} d\varphi\, M_3(\varphi) \int_{0}^{780} dz \int_{90\sec\varphi}^{\infty} S_3(z)\, e^{-0.0307(r-90)}\, r\, dr$$

$$+ \int_{3\pi/2-0.504}^{3\pi/2+0.594} d\varphi\, M_4(\varphi) \int_{0}^{780} dz \int_{163\sec\varphi}^{\infty} S_4(z)\, e^{-0.0307(r-163)}\, r\, dr.$$

8a. Cross Section for First 26 Feet

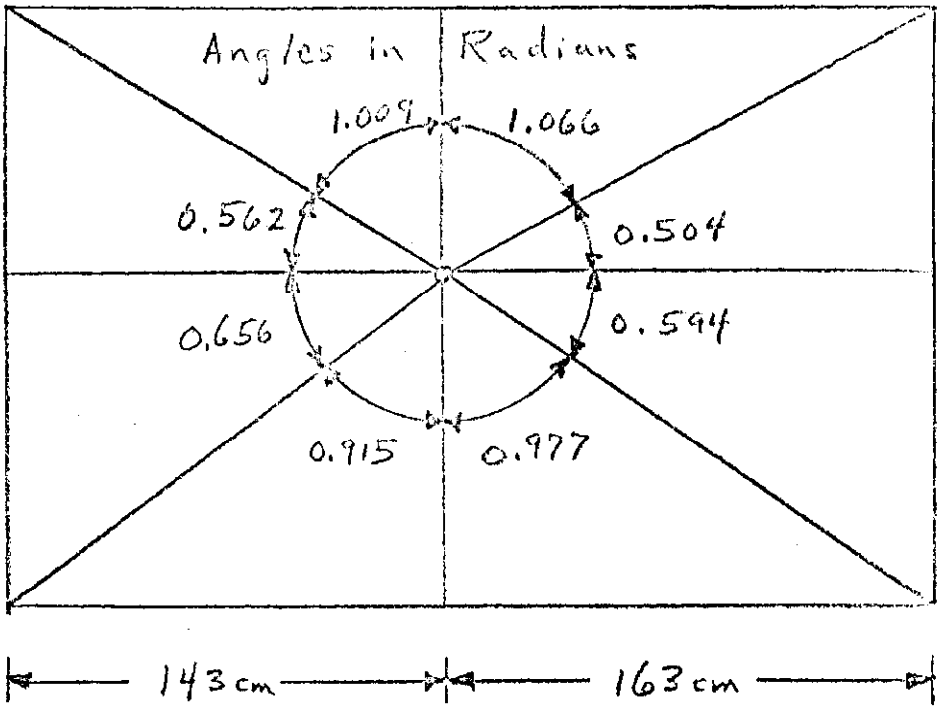

8b. Cross Section for Last 14 Feet

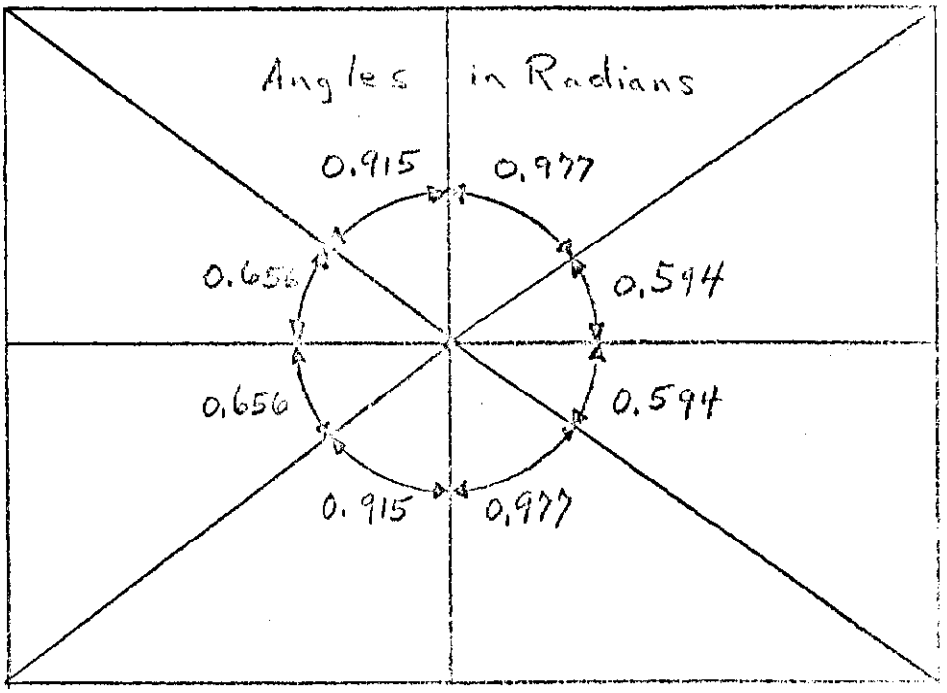

Figure 8. Equivalent Steel Blocks (Target Box Plus Concrete Enclosure

Since the source terms $S_j(z)$ are available every 60 cm (Table 2), the integral with respect to z becomes

$$\int_0^{780} dz\, S_j(z) = 60 \sum_{i=1}^{13} S_{ij}(z)$$

where $S_j(z)$ is evaluated at the beginning of the interval of length $\Delta z = 60$ cm. The last term is $S_{13}(720)$.

The individual terms were evaluated by making the change of variable $u = r - R_o(\varphi)$ in Equation 3 of the text. Hence,

$$\int_{R_o(\varphi)}^{\infty} e^{-0.0307\,[r - R_o(\varphi)]}\, r\, dr = \int_{u=0}^{\infty} e^{-0.0307 u}\, [u + R_o(\varphi)]\, du = \frac{1}{(0.0307)^2} + \frac{R_o(\varphi}{0.03}$$

Substituting from Table 2 the values for S_j and from Table A2.2 for M_j, I obtained $I_{0\text{-}26} = 216\,\mu Ci$

A3.2 Integration for the Last 14 Feet

The equations used for the last 14 feet of the target box ($780 \leq z < 1200$ cm) were as follows:

$$I_{26\text{-}40} = 2\int_{-0.977}^{0.915} d\varphi\, M_1(\varphi) \int_{z=780}^{z=1200} dz \int_{r=110\sec\varphi}^{\infty} S_1(z)\, e^{-0.0307(r-110)}\, r\, dr$$

$$+ \int_{\pi/2-0.656}^{\pi/2+0.656} d\varphi\, M_2(\varphi) \int_{z=780}^{z=1200} dz \int_{r=143\sec\varphi}^{\infty} S_2(z)\, e^{-0.0307(r-143)}\, r\, dr$$

$$+ \int_{3\pi/2-0.594}^{3\pi/2+0.594} d\varphi\, M_4(\varphi) \int_{z=780}^{z=1200} dz \int_{r=163\sec\varphi}^{\infty} S_4(z)\, e^{-0.0307(r-163)}\, r\, dr.$$

Substituting from Table 2 the values for S_i gave

$$I_{26-40} = 137 \mu C;$$

A3.3 Integration Beyond the End of the Target Box

The massive additional concrete shielding beyond the end of the target box insured that there was no soil activation for $z \geqq 1200$ cm and $r \leqq 110$ cm. An integration was still required to find the ^{22}Na activity for $r > 110$ cm. Since the last measured value of S(z) was for $z = 1140$ cm, an expression for S(z) was determined from that value for use when z was greater than 1200 cm. From the results of the Monte Carlo calculation (Fig. 3) I found that a decrease of ten times resulted for every 150 cm increase in z beyond $z = 1200$ cm. This yielded the expression

$$S(z) = S(1140) e^{-0.0154\,(z - 1200)} \qquad \text{for } z \geqq 1200.$$

Since the contribution to the total activity from beyond the end of the box was expected to be small, I simplified the calculation by assuming a cylindrical target box cross section of radius 110 cm, a conservative assumption. The resulting equation was

$$I_{>40} = \int_0^{2\pi} d\varphi \int_{z=1200}^{\infty} dz \int_{r=110}^{\infty} S_1(1140)\, e^{-0.0154\,(z-1200)}\, e^{-0.0307\,(r-110)}\, r\,dr$$

where the value S_1 (1140) corresponding to 110 cm of steel was used. The ^{22}Na activity in the soil beyond the end of the target box was

$$I_{>40} = 34 \mu C;$$

Since the activity decreases rapidly for $z < 0$ (Fig. 3) and since the calculation for $z > 1200$ was an over-estimate, no calculation was made for the activity in the soil preceding (upstream from) the target box. The total ^{22}Na activity in the soil, therefore, was

$$I_{total} = I_{0-26} + I_{26-40} + I_{>40}$$

or

$$I_{total} = 387\ \mu Ci$$

Appendix 4. CONVERSION TO DESIGN STEEL

Comparison with A. Van Ginneken's calculation for the Proton East Target Box[7] required changes in the steel thickness used in Appendix 3. The sides and bottom were 131 cm thick in the original design and the top was 109 cm. Since the integration (Appendix 3) was made for a steel thickness below the target of 110 cm, the values $S_1(z)$ were already available. These values for the ^{22}Na concentrations in the soil outside the concrete enclosure were determined from the tag results. The difference between 109 and 110 cm of steel resulted in only a three per cent correction for the concentration when a check was made at one location. Consequently, the values $S_1(z)$ were used in integrating the equation for the activity above the target box. The prescription used for the 131 cm thickness is given below.

To find the new set of concentrations $S_5(z)$ for a steel thickness of 131 cm, a new set of attenuation factors was needed. These were used to correct the values of $S_1(z)$ for use in the equations for the sides and bottom of the target box. Since the attenuation coefficients were known (Table A1.1) and the thickness difference was 131 - 110 or 21 cm, the attenuation factors were given by

$$f = e^{21/\mu}.$$

These factors and the new set of concentrations $S_5(z)$ are presented in Table A4.1.

Table A4.1. Attenuation Factors for Conversion to Design Steel

Distance Z from Front End of Target Box (cm)	Attenuation Coefficient μ	Attenuation Factor f	^{22}Na Soil Concentration Outside Wall	
			pCi/g	pCi/cm^3 S_5 (Z)
0	0.06978	4.33	0.44	1.1
60	"	"	0.85	2.1
120	0.04264	2.45	5.7	14
180	"	"	4.1	10
240	0.03838	2.24	3.5	8.5
300	"	"	2.8	6.7
360	"	"	2.1	4.9
420	"	"	2.1	4.9
480	"	"	1.3	3.1
540	"	"	0.63	1.5
600	"	"	0.63	1.5
660	"	"	1.1	2.5
720	"	"	2.1	9.8
780	"	"	2.2	10
840	"	"	1.3	6.3
900	"	"	0.67	3.1
960	"	"	1.2	5.8
1020	"	"	4.5	21
1080	"	"	4.2	20
1140	"	"	2.0	9.4

Since the design calculation by A. Van Ginneken[7] did not consider contributions from beyond the end of the target box, the integral from $z = 1200$ to ∞ was omitted. See Appendix 3. Also, since there was no change in thickness along the length of the box, the same equations were used for the entire length. Therefore, the equations used were simply

$$I_{0-40}^{\text{Design}} = 2\int_0^{\pi/2+0.698} d\varphi\, M_5(\varphi)\int_0^{1140} dz \int_{r=131}^{\infty} S_5(z)\, e^{-0.0307(r-131)}\, r\, dr$$

$$+ \int_{\pi-0.872}^{\pi+0.872} d\varphi\, M_1(\varphi)\int_0^{1140} dz \int_{r=109}^{\infty} S_1(z)\, e^{-0.0307(r-109)}\, r\, dr,$$

where the limits of integration for φ are shown in Fig. 7 and the values for $M_5(\varphi)$ are found in Table A2.3.

The result for the steel used in the design calculation was

$$I_{0-40}^{\text{Design}} = 313\,\mu\text{Ci}.$$